Ion Acoustic Turbulence in the Hollow Cathode Plume of a Hall Effect Thruster

Sarah E. Cusson*, Zachariah Brown†, Ethan T. Dale‡, Benjamin A. Jorns§, and Alec D. Gallimore¶
University of Michigan, Ann Arbor, MI, 48109

The ion acoustic turbulence in the plume of a hollow cathode operating in a Hall effect thruster is experimentally and analytically characterized. A recent theoretical study suggests that the increased resistivity as a result of the acoustic waves may dictate the cathode coupling voltage. The growth and strength of these waves are susceptible to changes in the neutral density or facility background pressure. A Langmuir probe is used to measure the steady state plasma parameters and wave properties with varying cathode flow fraction and background pressure. Results show that with increasing cathode flow fraction, the cathode coupling voltage decreases. Additionally, with increasing flow fraction, the electron temperature decreases. Both of these are consistent with lower ion acoustic turbulence strength. Ion saturation probes measure the wave properties. Results shows that the anomalous collision frequency grows with respect to the classical collision frequency with decreasing cathode flow fraction. This suggests that ion acoustic turbulence strength is correlated with the cathode coupling voltage in a Hall thruster for varying neutral density.

Nomenclature

$()_{e,i}$	=	electron, ion
A_p	=	Probe area [m^2]
A_s	=	Sheath area [m^2]
c_s	=	Ion sound speed [m/s]
i_{sat}	=	Ion saturation current [A]
k	=	wavenumver [1/m]
m	=	mass [kg]
n	=	density [1/m^3]
q	=	unit charge [C]
T_e	=	electron temperature [eV]
u_i	=	Ion drift speed [m/s]
V_{cc}	=	Cathode coupling voltage [V]
V_{cg}	=	Cathode to ground voltage [V]
V_f	=	floating potential [V]
V_p	=	plasma potential [V]
W	=	Wave energy density [J/m^3]
ϕ	=	potential [V]
ω_0	=	cutoff frequency [Hz]
ω_p	=	plasma frequency [Hz]
ν_{an}	=	anomalous collision frequency [Hz]
ν_{ei}	=	Coulomb collision frequency [Hz]

*Ph.D. Candidate, Department of Aerospace Engineering, and AIAA Student Member
†Ph.D. Candidate, Department of Aerospace Engineering, and AIAA Student Member
‡Ph.D. Candidate, Department of Aerospace Engineering, and AIAA Student Member
§Assistant Professor, Department of Aerospace Engineering, and AIAA Senior Member
¶Robert J. Vlasic Dean of Engineering, College of Engineering, and AIAA Fellow

I. Introduction

Ion acoustic turbulence is known to impact the behavior of hollow cathodes. The instability is thought to be the dominant mechanism driving the plasmadynamics in this region. Previous works have confirmed their existence in the plume of stand-alone hollow cathodes and derived a self-consistent fluid model for wave energy transport[1, 2]. The numerical model OrCa2D, a first-principles fluid model for cathodes developed by the Jet Propulsion Laboratory (JPL), showed significant improvement in experimental agreement after incorporating ion acoustic turbulence based on Sagdeev's formulation[3] into the code[4]. They refer to this ion acoustic turbulence as an "anomalous collision frequency" since it is not a collision driven process. Additionally, when this anomalous collision frequency was implemented into JPL's full thruster simulation code, Hall2De, simulations showed closer agreement to the experimental data in the near-field plume[5]. Therefore, it is apparent that the anomalous collision frequency is critical to capturing the plasmadynamics of the cathode region in a Hall thruster.

Although Hall thrusters have decades of flight history[6, 7], there still remain fundamental questions about their operation. One of the most pressing issues is their performance in space versus ground test facilities. Studies have shown a cross-cutting susceptibility to variation in performance due to background pressure changes[8–14]. However, the mechanism behind these so-called "facility effects" remains unidentified. While testing facilities impacts multiple thruster parameters, here we focus on one: the change in magnitude of the cathode coupling voltage. The cathode coupling voltage, V_{cc}, is generally defined as the voltage between the cathode and the plume of the Hall thruster. It is associated with the ease with which electrons travel from the cathode into the thruster. Previous studies[10] have shown that the magnitude of the cathode coupling voltage increases with decreasing background pressure.

The central hypothesis presented here is that ion acoustic turbulence exists in the plume of a hollow cathode operating in a Hall thruster and is critical to the cathode coupling voltage. This turbulence manifests by taking energy from the electron drift velocity and redistributing it into the electron thermal energy and ion kinetic and thermal energy[2]. In practice, most of the energy is redistributed into the thermal energy of both species. This, in turn, demands more work from the electrons to couple to the thruster channel. Neutral density has theoretically been shown to impact the coupling voltage through damping of the ion acoustic turbulence[15], however no experimental investigation has confirmed the existence of these waves in a hollow cathode operating in a Hall thruster. Additionally, there is no experimental evidence that there exists a mechanism to drive variations in the turbulence with varying neutral density (background pressure). Therefore, the need is apparent for an experimental investigation to characterize the physics of ion acoustic turbulence in the hollow cathode of an operating Hall thruster with varying neutral density.

In order to accomplish this investigation, this paper is structured as follows: first, we present a discussion of ion acoustic turbulence theory. Then, we detail the experimental apparatus used to measure the ion acoustic turbulence and steady-state plasma parameter in the hollow cathode plume. We then present the results of the study as well as a discussion of these results. Finally, we draw conclusions based on the results regarding the impact of ion acoustic turbulence on the hollow cathode plume and the coupling voltage of a Hall thruster.

II. Ion Acoustic Turbulence Theory

In this section, we present the theory for ion acoustic turbulence in a hollow cathode that has previously been developed by Jorns[2]. First, we examine the energy density of these waves and then relate this to an anomalous collision frequency. Then, we present a discussion of these waves in the context of neutral density and cathode coupling. Ion acoustic turbulence is commonly found in current-carrying plasmas and is associated with an increased plasma resistivity[16]. This increased resistivity typically takes the form of an effective (anomalous) collision frequency. In general, ion acoustic turbulence consists of a spectrum of electrostatic waves with random phases in a plasma. It is the summation of acoustic modes that are closely spaced in frequency and excited concurrently in the same region. All of these waves must adhere to the dispersion relation in order to propagate undamped. For ion acoustic waves, the dispersion relates frequency to wavelength according to $\omega = k(c_s + u_i)$, where c_s is the ion sound speed and u_i is the ion drift speed.

We can calculate the total wave energy density of the acoustic waves by summing the energy density of each mode over frequency space as[2, 17],

$$W = \frac{n_e}{T_e}\sum_{\omega_0}^{\omega_{pi}}[q\phi(\omega)]^2 \tag{1}$$

where W is the wave energy density, ω_{pi} is the ion plasma frequency, and ω_0 is the cutoff frequency. The lower bound in Equation 1 is the frequency below which we do not expect to see ion acoustic turbulence and thus accounting for lower frequencies would include contributions not associated with ion acoustic turbulence. This cutoff is associated with ion-neutral damping[2]. This method was previously employed by Dodson[18] and Jorns[1]. Here, the cutoff frequency is taken as 200 kHz. The high frequency cutoff represents a departure from linear growth and is thought to be the result of non-linear saturation such as electron trapping[19], ion resonance broadening[20, 21] or non-linear ion Landau damping[22].

The anomalous collision frequency due to ion acoustic turbulence can be approximated via weak-turbulent theory described by Sagdeev and Galeev[3]. Under the assumption that the damping at high frequency is the result of non-linear ion Landau damping[1], this formulation is

$$\nu_{an} = \alpha\frac{\omega_{pe}W}{nT_e} \tag{2}$$

where ω_{pe} is the electron plasma frequency, and α is an empirically driven constant found to be $O(10^{-2})$. Assuming that the waves are one-directional with the electron drift[23], we can substitute Equation 1 into Equation 2 to get,

$$\nu_{an} = \frac{\alpha\omega_{pe}}{T_e^2}\sum_{\omega}^{\omega_{pi}}[q\phi(\omega)]^2 \tag{3}$$

Previous work[1] has shown that neutral-ion collisions act to damp the growth of these modes. At constant current, there should be more neutral-ion collisions with increasing neutral density without affecting the growth from inverse Landau damping of electrons. Saturation of these waves occurs when the damping terms balance the growth terms. Increasing the neutral density should increase the neutral damping and therefore lower the wave energy density amplitude[23]. In turn, as the neutral density increases, the ion acoustic turbulence should decrease[23]. Since the ion acoustic turbulence takes energy from the electron drift, an increase in the energy density would slow the electrons more. This should make it harder for electrons to travel from the cathode to the thruster plume. Therefore, we expect that as the total wave energy density increases, the voltage required to extract electron from the cathode, V_{cc}, should increase. Bringing this all together, this would indicate that we should expect the cathode coupling voltage to increase as the neutral density decreases due to increasing turbulent energy.

In order to experimentally investigate this, we thus look for evidence of ion acoustic turbulence in the hollow cathode of an operating in a Hall thruster. Additionally, we aim to look at the variation in wave energy density and cathode coupling change with neutral density.

III. Experimental Apparatus

This section outlines the experimental apparatus used to obtain cathode coupling voltage and wave energy density measurements.

A. Thruster

We used the H9 Hall thruster for this experiment. The thruster is a single channel magnetically shielded Hall thruster jointly developed by NASA's Jet Propulsion Laboratory, the University of Michigan and the Air Force Research Laboratory[24, 25]. The thruster has a nominal power level of 9 kW and a similar design to other state-of-the art Hall thrusters. During this campaign, the thruster was run at a power level of 4.5 kW, which is within its nominal throttling curve. The thruster was in the cathode-tied electrical configuration and was run off a centrally-mounted LaB_6 cathode. A picture of the thruster installed in the facility can be seen in Figure 1. Additionally, the probes discussed in Sections IIIC and IIID can be seen mounted to the motion stages in the figure. The anode and cathode were supplied with research-grade xenon through commercially available mass flow controllers.

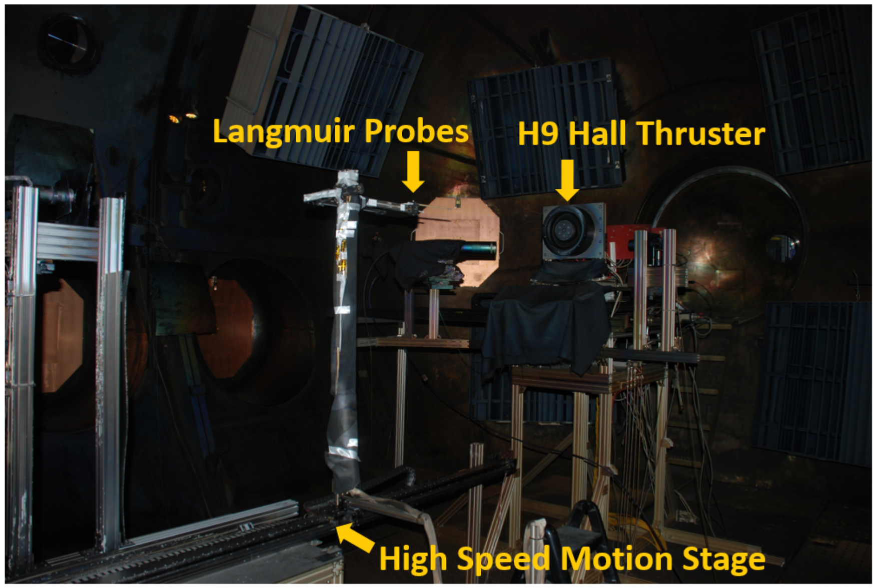

Fig. 1 The H9 Hall thruster installed in the Large Vacuum Test Facility. The probes mounted to the high speed motion stage are in in the foreground.

B. Facility
All testing occurred in the Large Vacuum Test Facility (LVTF) at the University of Michigan. LVTF is a 9 meters long, 6 meters diameter vacuum chamber with a base pressure of 5×10^{-7} Torr-Xe. Pressure was measured using a Stabil Ion gauge located approximately 1 meter away from the thruster in line with the exit plane. The gauge has a grounded mesh attached to the entrance per industry standard [26]. The chamber was equipped with two stepper motor motion stages to adjust the position of thruster relative to probes, and a linear induction motion stage capable of high speed axial probe injection.

C. Langmuir Probe
We employed a planar Langmuir probe to measure electron temperature, plasma potential, and density. The bias voltage was swept from -25 V to 25 V using a Krohn-Hite 7500 wideband amplifier set to 10X gain and driven with a GW Instek AFG-2225 function generator. Current was sensed using a Tektronix current gun that was read by a 16-bit AlazarTech ATS9462 waveform digitizer. In order to calculate the plasma potential, we first calculated the numerical derivative (dI/dV) of the I-V trace. The plasma potential is the voltage corresponding to the peak value in this numerical derivative. Electron temperature was calculated as[27],

$$T_e = \frac{V_p - V_f}{\ln\left(\sqrt{\frac{m_i}{2\pi m_e}}\right)} \tag{4}$$

where V_f is the floating potential (potential where the trace is closest to zero), m_i is the mass of a xenon ion and m_e is the mass of an electron. Finally, the density is calculated as,

$$n_e = -\exp(1/2)\frac{i_{sat}}{qA_s}\sqrt{\frac{m_i}{qT_e}} \tag{5}$$

where i_{sat} is the probe current at ion saturation and A_s is the area of the sheath. Here, we use the thin-sheath assumption ($A_s \approx A_p$).

D. Wave Probes
In order to measure the plasma waves, we employed two closely spaced cylindrical Langmuir probes set to collect ion saturation current. The probes were biased to a constant voltage of -36V using batter-

ies. The time-resolved current was inferred by measuring the voltage drop across a 100 Ohm low inductance metal foil resistor with another 16-bit ATS9462 analog waveform digitizer with a 65 MHz bandwidth. In order to obtain wave properties, a cross-correlation between the two probes was performed to determine the dispersion of the plasma[2, 23]. Specifically, the Beall method analysis was used to produce wave intensity plots of wavenumber vs frequency. The vector between the two probes defined the directional component of the wave being measured[28]. The power density traces were places into 10 kHz bins to reduce noise in the high frequency spectrum. The probes were spaced 5.5 mm apart for axial measurements. We binned the cross-correlation values into wavenumber bins of 8 rads/m. Additionally, for low amplitude (i.e. $\tilde{\phi} << T_e$) electrostatic waves, we related the potential fluctuations as[2],

$$\tilde{\phi} = \frac{T_e}{q}\frac{\tilde{n}}{n} \tag{6}$$

where $\tilde{n}$ are fluctuations in the plasma density. Under the assumptions that electron temperature fluctuations are small, the relative fluctuations in density should equal those in ion saturation current collected from the probe. This allows us to re-write Equations 6 as,

$$\tilde{\phi} = \frac{T_e}{q}\frac{\tilde{i}_{sat}}{i_{sat}} \tag{7}$$

where i_{sat} is the mean ion saturation current collected. A picture of the probes can be seen in Figure 2. In this campaign, we investigated the near-field of the cathode plume. We swept the probes radially from thruster centerline to channel centerline and axially from 1.5 to 4 cm downstream of the thruster exit plane with 2.5 mm resolution. Ion saturation current measured in the near field grid was sampled the signal at 10MS/s. The two probes were synced and over 1 million samples were taken per trace.

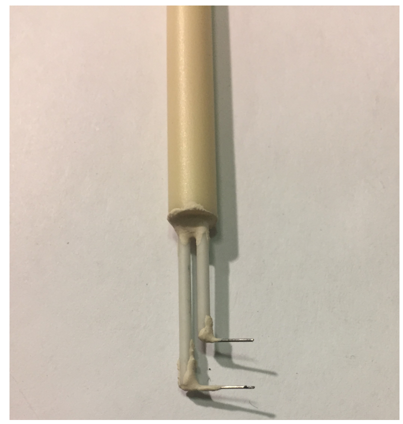

Fig. 2 Ion saturation probes employed to measure the plasma waves.

E. Test Matrix

We operated the thruster at five different test points detailed in Table 1. The discharge voltage for the thruster was 300 V for all conditions, and the discharge current was 15 A. The thruster was run for 3.5 hours and above the experimental operating power prior to any measurements being taken in order to ensure the thruster was fully “baked-out". Test point 2 was completed first. In order to vary the neutral density in the plume of the cathode, we varied to cathode flow fraction. The cathode flow fraction is taken as the percent of anode flow. For the study, no flow was injected into the background and the fraction was varied from 5% to 15%.

Test Point	Power (kW)	Pressure (Torr-Xe)	Cathode Flow Fraction
1	4.5	7×10^{-6}	5%
2	4.5	7×10^{-6}	7%
3	4.5	7×10^{-6}	10%
4	4.5	7×10^{-6}	12.5%
5	4.5	7×10^{-6}	15%

IV. Results

In this section, we present the results of the experiment. First, we look for evidence that ion acoustic waves exist in the plume of the hollow cathode. Next, we present and discuss the properties of these waves. Finally, we present the steady plasma parameters and discuss them in the context of expectations based on ion acoustic turbulence.

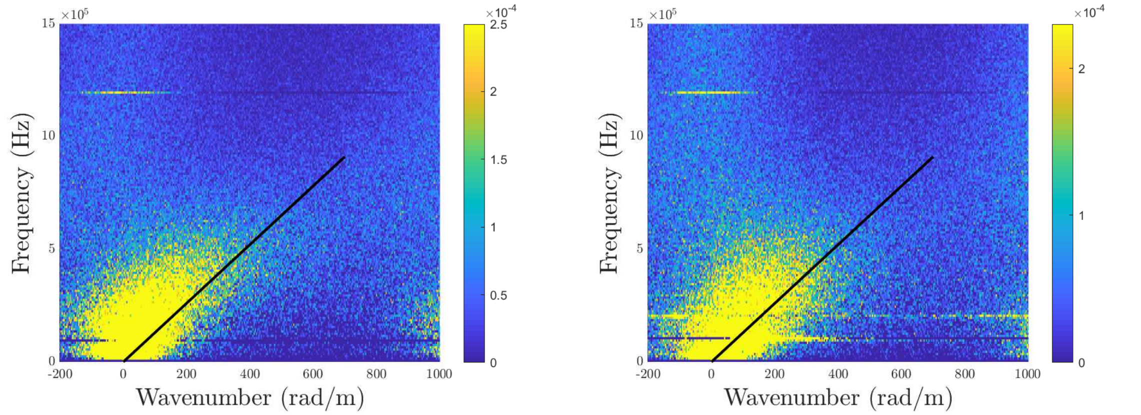

(a) Example Beall plot showing the acoustic like nature of the waves at the 7% cathode flow fraction condition 3 centimeters downstream.

(b) Example Beall plot showing the acoustic like nature of the waves at the 5% cathode flow fraction condition 3 centimeters downstream.

Fig. 3

A. Wave Measurements

First and foremost, we investigated whether ion acoustic turbulence is present in the plume of a hollow cathode operating in a Hall thruster. To do this, we look at the estimated dispersion of the plasma using the Beall technique[28]. Figures 3a and 3b show examples of this plot for the 5% and 7% CFF conditions 3 centimeters downstream of the thruster. The frequency appears to depend linearly on the wave number (black line superimposed on a plot) which is the dispersion expected for acoustic like waves. Taking the slope of the line in Figure 3a, the calculated phase velocity is 4.7 km/s after accounting for oblique propagation. We calculate the ion sound speed ($\sqrt{qT_e/m_i}$) for this case to be 1.8 km/s. This would result in a ion drift speed of approximately 3 km/s which is commensurate with drift speeds seen in literature[2, 29]. Based on these results and plots, there is strong evidence of the existence of acoustic-like waves in the hollow cathode plume of an operating Hall thruster. This is the first measurement that we know of that confirms these waves. Next, we attempt to quantify these waves and their dependence on neutral density. First, we look at the amplitude of the potential fluctuations as defined by Equation 7.

Figure 4 shows an example of these fluctuations versus frequency for varying cathode flow fraction. These data are taken 1.5 centimeters downstream from the cathode. Qualitatively, we see that the overall spectrum of oscillations remains the same across all traces. There is low frequency content, generally associated with global oscillations of the cathode and the anode. The anode oscillations are referred to as the "breathing mode" and generally range between 10 to 30 kHz[30]. The cathode oscillations are generally associated with a "cathode spoke" ranging from 70 to 100 kHz[31]. The strength of these oscillations is independent of cathode flow fraction. However, the high frequency oscillations (above 200 kHz) appear to grow in strength as the cathode flow fraction increases. This would suggest that an increased neutral density is damping the strength of the higher frequency content. This result was previously observed by Jorns for a stand alone cathode[2]. There appears to be a spike at 1.2 MHz, however this was taken as noise because the spike is dispersion-less and the same magnitude (un-normalized) across all conditions. Additionally, there is a broad peak around 2.7 MHz. This is likely associated with channel-born oscillations[32].

Next, we aim to calculate the total wave energy density and change in plasma collisionality due to the changing strength of potential fluctuations. First, however, we must calculate the global plasma parameters. Using Equations 4 and 5, and the Langmuir probe I-V sweeps, we calculate the spatial evolution of the electron temperature and density. These values are then coupled into Equations 1 through 3 and Equations 6 and 7 to calculate the wave properties.

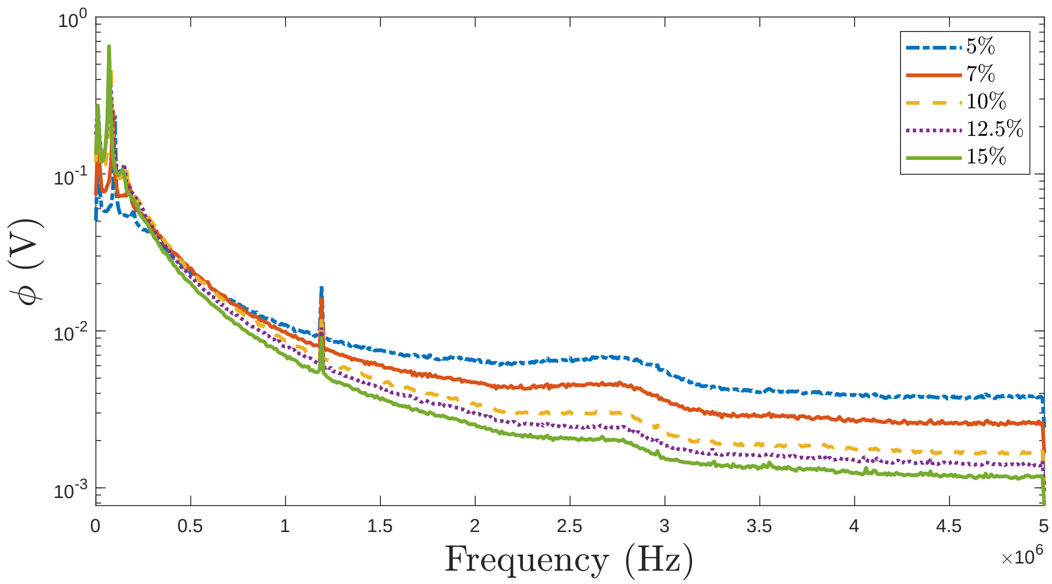

Fig. 4 Potential fluctuations as a function of frequency for varying cathode flow fractions.

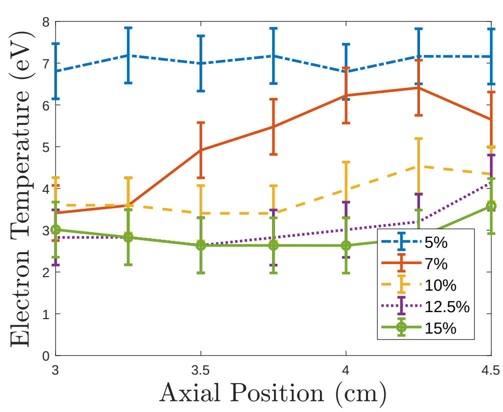

(a) Spatial evolution of electron temperature versus cathode flow fraction.

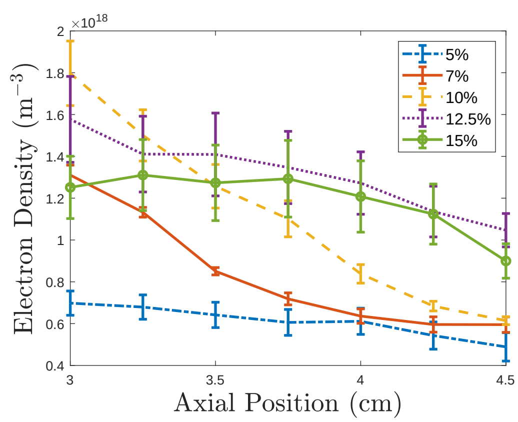

(b) Spatial evolution of electron density versus cathode flow fraction

Fig. 5

Figure 5a shows the spatial evolution of the electron temperature for each cathode flow fraction. The results show that, in general, the electron temperature increases with increasing axial distance from the cathode. These results support the theory of ion acoustic turbulence as the waves are thought to take kinetic energy from the electrons and deposit it into the thermal energy of electrons and ions. However, this could be due to Ohmic heating as well. Additionally, the electron temperature in all spatial locations increases with decreasing flow fraction. This result also supports the existence of ion acoustic waves as neutral density should damp the waves, therefore reducing the amount of energy available to deposit into the thermal states. The electron density as a function of position and cathode flow fraction is shown in Figure 5b. The results show that the density is of similar order of magnitude for all cases, as expected since the total current the cathode is providing does not vary between conditions.

We now look at the results from calculating the wave energy density and anomalous collision frequency with respect to position for varying cathode flow fractions. These results are seen in Figures 6a and 6b. There are two points of interest in the fluctuation strength plot: (1) the peak value increases with decreasing flow fraction and (2) the waves peak closer to the cathode with decreasing flow fraction. In Figure 6b, we see that the collision frequency appears to decrease as a function of position. Additionally, the values for collision frequency seen here are of the same order of magnitude previously reported[4].

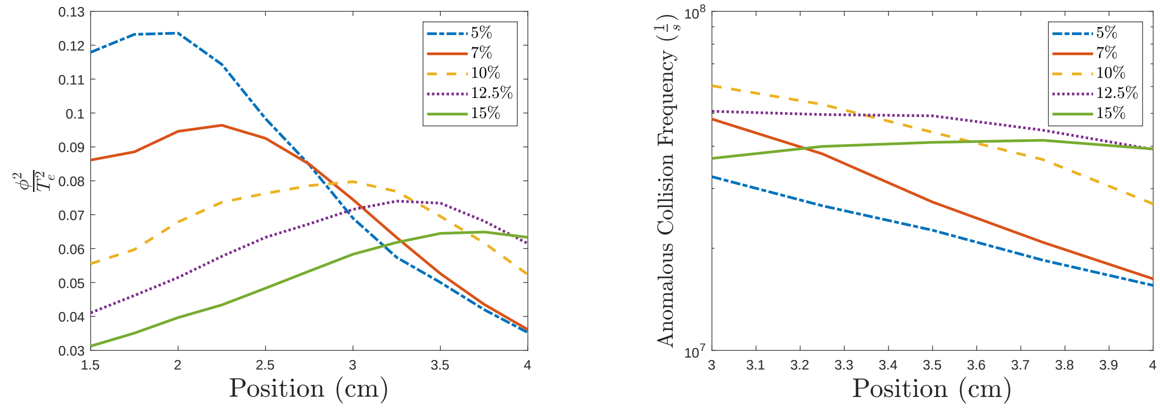

(a) Relative strength of oscillation as a function of position for each cathode flow fraction case.

(b) Anomalous collision frequency due to ion acoustic turbulence for each cathode flow fraction case.

Fig. 6

V. Discussion

In this section, we discuss the results presented above in the context of dominance in the plume and the impact on the thruster operation.

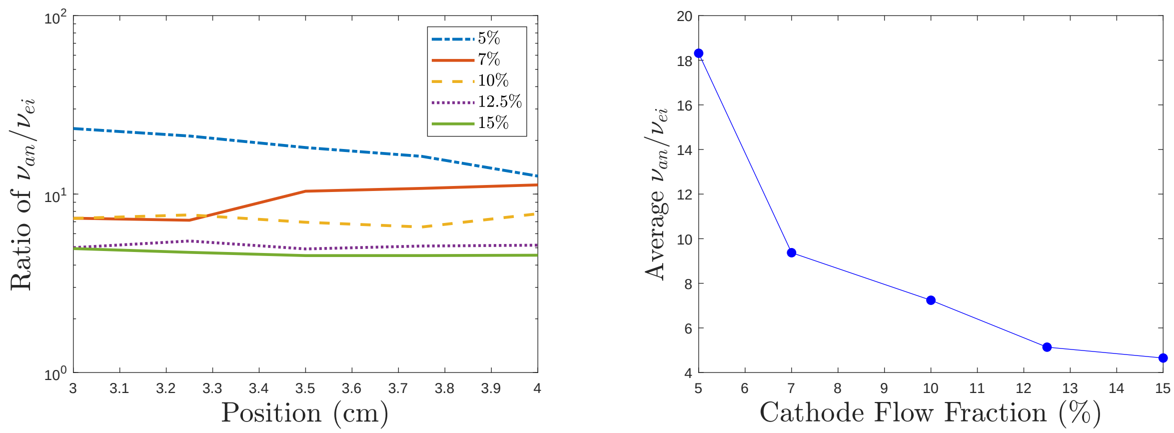

(a) Ratio of collision frequency due to ion acoustic turbulence and classical Coulomb collisions.

(b) Average ratio of collision frequency due to ion acoustic turbulence and classical Coulomb collisions as a function of cathode flow fraction.

Fig. 7

Figure 6b shows the total effective collision frequency due to ion acoustic turbulence. However, it is impossible to frame these results without comparing them to the classic collision frequencies. If, these effective frequencies are orders of magnitude smaller than classically expected, then we would not expect ion acoustic turbulence to play an important role in this region. However, if they are an appreciable fraction or larger than classically expected, that would indicate that ion acoustic turbulence is important to consider in the plasmadynamics of the region. We calculate the classical collision frequency as the Coulomb collision frequency. The formulation for this is[33],

$$\nu_{ei} = 2.9 \times 10^{-12} \frac{n_e}{T_e^{3/2}} \left[23 - \frac{1}{2} \log \left(\frac{10^{-6} n_e}{T_e^3} \right) \right] \tag{8}$$

Now, we take the ratio of the anomalous collision frequency calculated by Equation 3 and shown in Figure 6b and the classically expected collision frequency in Equation 8. The results of this are seen in Figure 7a.

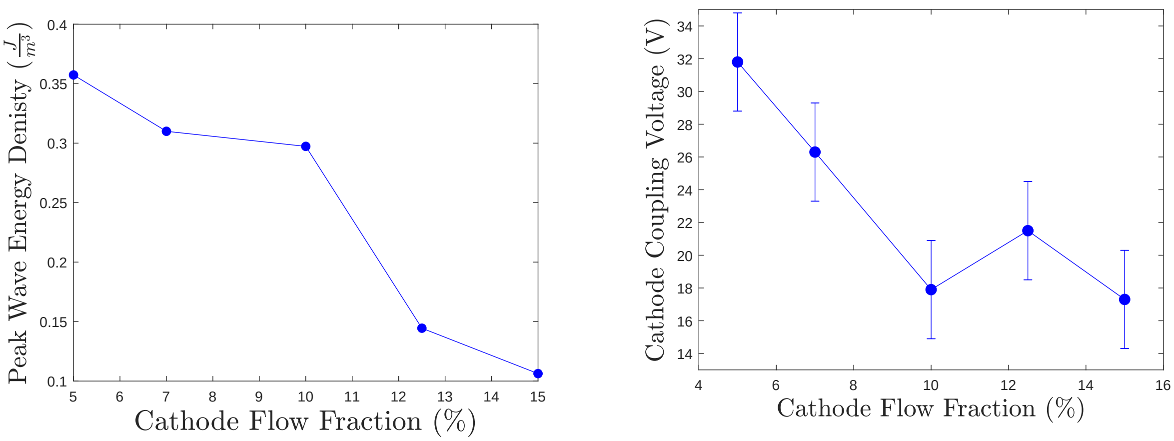

(a) Peak wave energy density in the plume of the cathode as a function of cathode flow fraction.

(b) Cathode Coupling Voltage as a function of cathode flow fraction.

Fig. 8

The results show that as the cathode flow fraction is decreased, the relative importance of the ion acoustic turbulence increases. In other words, the ion acoustic turbulence begins to dominate the electron collision frequency to a higher extent. In Figure 7b, we plot the spatial average of the ratios of collision frequencies as a function of cathode flow fraction. We observe that as the cathode flow fraction increases, this value approaches one. This indicates that the changing dynamics of plasma properties with varying cathode flow fraction are dominated by the ion acoustic turbulence resistivity.

Additionally, if we look at Figures 8a and 8b, we see the peak wave energy and corresponding cathode coupling voltage ($V_{cc} = V_p - V_{cg}$). Figure 8a shows that as cathode flow fraction is increased, the peak wave energy density decreases. This would suggest that the ion-neutral damping term is increasing with increasing cathode flow fraction, as expected. This is likely caused by a lower saturation wave energy or lower amount of turbulence. The saturation wave energy depend on the electron temperature[23], therefore as T_e decreases with flow fraction, so does the peak wave energy. This, in turn, suggests that the amount of turbulence in the plume decreases yielding higher resistivity decreases. This is supported by Figure 8b, which shows that the total coupling voltage of the thruster decreases with increasing flow fraction. Therefore, there is a clear correlation between wave energy density and cathode coupling voltage in the plume of a hollow cathode.

VI. Conclusions

We aimed to experimentally investigate the presence of ion acoustic turbulence in the plume of a hollow cathode operating in a Hall thruster. We measured the waves using two ion saturation probes. First, we proved the existence of ion acoustic waves in the hollow cathode plume operating in a Hall thruster. We then showed that the relative strength of the collision frequency as compared to classical collision frequencies grows as neutral density drops. Additionally, we showed that both the peak wave energy density and the total thruster coupling voltage decrease with increasing cathode flow fraction. Therefore, we concluded that neutral density drops in the plume of a hollow cathode may increase the strength of ion acoustic turbulence therefore increasing the coupling voltage. Particularly for externally mounted hollow cathodes, this would suggest that the changes observed in coupling versus background pressure are due to the onset of ion acoustic turbulence.

Acknowledgments

The authors would like to thank the entirety of the Plasmadynamics and Electric Propulsion Laboratory for their assistance and advice throughout the duration of the experiment. The authors would like to acknowledge funding provided by the NASA Space Technology Research Fellowship grant numbers NNX15AQ43H and NNX14AL65H, NSF GRFP grant number DGE 1256260 and AFOSR grant number FA9550-17-1-0035.

References

[1] Jorns, B., Lopez Ortega, A., and Mikellides, I. G., "First-principles modelling of the IAT-driven anomalous resistivity in hollow cathode discharges I: Theory," *52nd AIAA/SAE/ASEE Joint Propulsion Conference*, 2016, p. 4626.

[2] Jorns, B. A., Mikellides, I. G., and Goebel, D. M., "Ion acoustic turbulence in a 100-A LaB 6 hollow cathode," *Physical Review E*, Vol. 90, No. 6, 2014, p. 063106.

[3] Sagdeev, R. Z., and Galeev, A. A., "Nonlinear plasma theory," *Nonlinear Plasma Theory, New York: Benjamin, 1969*, 1969.

[4] Lopez Ortega, A., Mikellides, I. G., and Jorns, B., "First-principles modeling of the IAT-driven anomalous resistivity in hollow cathode discharges II: Numerical simulations and comparison with measurements," *52nd AIAA/SAE/ASEE Joint Propulsion Conference*, 2016, p. 4627.

[5] Lopez Ortega, A., and Mikellides, I. G., "The importance of the cathode plume and its interactions with the ion beam in numerical simulations of Hall thrusters," *Physics of Plasmas*, Vol. 23, No. 4, 2016, p. 043515.

[6] Morozov, A., "The conceptual development of stationary plasma thrusters," *Plasma Physics Reports*, Vol. 29, No. 3, 2003, pp. 235–250.

[7] Morozov, A., and Savelyev, V., "Fundamentals of stationary plasma thruster theory," *Reviews of plasma physics*, Springer, 2000, pp. 203–391.

[8] Randolph, T., Kim, V., Kaufman, H., Kozubsky, K., Zhurin, V., and Day, M., "Facility effects on stationary plasma thruster testing," *23rd International Electric Propulsion Conference*, 1993, pp. 1993–093.

[9] Hofer, R. R., and Anderson, J. R., "Finite Pressure Effects in Magnetically Shielded Hall Thrusters," *50th AIAA/ASME/SAE/ASEE Joint Propulsion Conference*, 2014, p. 3709.

[10] Huang, W., Kamhawi, H., and Haag, T., "Facility effect characterization test of NASA's HERMes Hall thruster," *52nd AIAA/SAE/ASEE Joint Propulsion Conference*, 2016, p. 4828.

[11] Nakles, M., and Hargus, W., "Background pressure effects on internal and near-field ion velocity distribution of the BHT-600 Hall thruster," *44th AIAA/ASME/SAE/ASEE Joint Propulsion Conference & Exhibit*, 2008, p. 5101.

[12] Hofer, R. R., Peterson, P. Y., and Gallimore, A. D., "Characterizing vacuum facility backpressure effects on the performance of a Hall thruster," IEPC-01-045, 27th International Electric Propulsion Conference, Pasadena, CA, 2001.

[13] Huang, W., Kamhawi, H., and Haag, T., "Effect of background pressure on the performance and plume of the hivhac hall thruster," 2013.

[14] Spektor, R., and Tighe, W. G., “Laser Induced Fluorescence Measurements in a Hall Thruster as a Function of Background Pressure,” *52nd AIAA/SAE/ASEE Joint Propulsion Conference*, 2016, p. 4624.

[15] Cusson, S. E., Jorns, B., and Gallimore, A., “Simple Model for Cathode Coupling Voltage Versus Background Pressure in a Hall Thruster,” *53rd AIAA/SAE/ASEE Joint Propulsion Conference*, 2017, p. 4889.

[16] Horton, C. W., and Horton, W., *Turbulent transport in magnetized plasmas*, World Scientific, 2012.

[17] Stix, T., “Plasma waves,” *A. I. P., New York*, 1992.

[18] Dodson, C., Perez-Grande, D., Jorns, B., Goebel, D. M., and Wirz, R. E., “Laser-induced fluorescence measurements of energetic Ions in a 100-A LaB6 hollow cathode plume,” *52nd AIAA/SAE/ASEE Joint Propulsion Conference*, 2016, p. 4838.

[19] Nishikawa, K., and Wu, C.-S., “Effect of electron trapping on the ion-wave instability,” *Physical Review Letters*, Vol. 23, No. 18, 1969, p. 1020.

[20] Sleeper, A. M., Weinstock, J., and Bezzerides, B., “Nonlinear theory and angular spectrum of the ion-acoustic instability,” *The Physics of Fluids*, Vol. 16, No. 9, 1973, pp. 1508–1518.

[21] Basu, A., Sharma, A. S., and Das, A., “Spectrum of turbulent ion acoustic waves in a magnetic field,” *Plasma physics and controlled fusion*, Vol. 27, No. 4, 1985, p. 433.

[22] Kadomtsev, B. B., “Plasma turbulence,” *New York: Academic Press, 1965*, 1965.

[23] Jorns, B. A., Dodson, C., Goebel, D. M., and Wirz, R., “Propagation of ion acoustic wave energy in the plume of a high-current LaB 6 hollow cathode,” *Physical Review E*, Vol. 96, No. 2, 2017, p. 023208.

[24] Hofer, R. R., Cusson, S. E., Lobbia, R. B., and Gallimore, A. D., “The H9 Magnetically Shielded Hall Thruster,” *35th International Electric Propulsion Conference*, Atlanta,GA, 2017.

[25] Cusson, S. E., Hofer, R. R., Lobbia, R. B., Jorns, B. A., and Gallimore, A. D., “Performance of the H9 Magnetically Shielded Hall Thrusters,” 2017.

[26] Dankanich, J. W., Walker, M., Swiatek, M. W., and Yim, J. T., “Recommended Practice for Pressure Measurement and Calculation of Effective Pumping Speed in Electric Propulsion Testing,” *Journal of Propulsion and Power*, 2016.

[27] Lobbia, R. B., and Beal, B. E., “Recommended Practice for Use of Langmuir Probes in Electric Propulsion Testing,” *Journal of Propulsion and Power*, 2017, pp. 1–16.

[28] Beall, J., Kim, Y., and Powers, E., “Estimation of wavenumber and frequency spectra using fixed probe pairs,” *Journal of Applied Physics*, Vol. 53, No. 6, 1982, pp. 3933–3940.

[29] Williams, G. J., Smith, T. B., Domonkos, M. T., Gallimore, A. D., and Drake, R. P., “Laser-induced fluorescence characterization of ions emitted from hollow cathodes,” *IEEE Transactions on Plasma Science*, Vol. 28, No. 5, 2000, pp. 1664–1675.

[30] Choueiri, E., “Plasma oscillations in Hall thrusters,” *Physics of Plasmas*, Vol. 8, No. 4, 2001, pp. 1411–1426.

[31] Jorns, B. A., and Hofer, R. R., “Plasma oscillations in a 6-kW magnetically shielded Hall thruster,” *Physics of Plasmas*, Vol. 21, No. 5, 2014, p. 053512.

[32] Brown, Z. A., and Jorns, B. A., “Spatial Evolution of Plasma Waves in the Acceleration Region and Near Field of a Magnetically Shielded Hall Thruster,” *54th AIAA/SAE/ASEE Joint Propulsion Conference*, 2018.

[33] Goebel, D. M., and Katz, I., *Fundamentals of Electric Propulsion: Ion and Hall Thrusters*, Vol. 1, John Wiley & Sons, 2008.